Department of Cardiology[1], Beijing Friendship Hospital, Capital Medical University; Beijing Key Laboratory of Metabolic Disorder Related Cardiovascular Disease[2], Beijing, China

Nicorandil protects cardiac microvascular endothelial cells from advanced glycation end products induced cytotoxicity via promoting autophagy

Bing Hua[1], Hehe Cui[1,*], Qingbo Liu[1], Weiping Li[1,2], Hui Chen[1], Hongwei Li[1,2,*]

Received September 26, 2020, accepted October 30, 2020

**Corresponding authors: Hehe Cui, Hongwei Li, Department of Cardiology, Beijing Friendship Hospital, Capital Medical University. No.95 Yong'An Road, Xicheng District, Beijing 100050, China*
cuihh@126.com
lhw19656@sina.com

Pharmazie 76: 18-22 (2021) *doi: 10.1691/ph.2021.0831*

Microvascular dysfunction, as a major comorbidity of Diabetes mellitus, is mainly induced by advanced glycation end products (AGEs). We hypothesized that the anti-angina medicine nicorandil protects cardiac microvascular endothelial cells (CMECs) subjected to AGEs and investigated the mechanisms regarding to autophagy regulation. Cellular viability and migration were analyzed to determine the effects of nicorandil or pathway inhibitors. Western blot, monodansylcadaverine (MDC) staining, adenovirus expressing mCherry – green fluorescent protein light chain 3 (LC3) transfection, transmission electron microscopy and confocal microscopy were used to elucidate autophagy and its regulation. Nicorandil at 100 μM ameliorated the AGE-induced cytotoxicity. LC3-II upregulation and increased autophagosome formation were found in the nicorandil-treated groups compared with the AGE groups, which were suppressed by wortmannin or chloroquine. Wortmannin or chloroquine attenuated cellular protection of nicorandil. AGEs promoted phosphorylation of IκB kinase β (IKKβ), IκBα and p65, the target proteins in the nuclear factor-kappa B (NF-κB) signaling pathway. Inactivating the NF-κB pathway by pyrrolidine dithiocarbamate (PDTC) or nicorandil increased the level of LC3-II or the formation of MDC-labeled autophagosome. Confocal microscopy revealed that nicorandil as well as PDTC promoted autophagic flux in AGEs treated CMECs. The study suggests that nicorandil exerts cytoprotective effects on CMECs from AGEs by inducing autophagy, partly through inhibiting the NF-κB signaling pathway.

1. Introduction

Advanced glycation end products (AGEs), a group of compounds produced by reducing sugars and amine residues via non-enzymatic reaction, are well recognized pathogenic mediators in Diabetic mellitus (DM) (Chaudhuri et al. 2018). AGEs play a pivotal role in promoting diabetic microvascular complications (Yang et al. 2019). Autophagy (more accurately, macroautophagy) is a lysosome-mediated cellular response that involves the sequestration of cytoplasmic components in autophagosomes (Choi et al. 2013). The cellular self-digestion process regulating damaged organelles and misfolded proteins degeneration is essential for cell survival and maintenance of cellular homeostasis, which is hampered in type 2 DM (Ravikumar et al. 2010).

Some evidence indicated that upregulating autophagy in human umbilical vein endothelial cells (HUVECs) protected against AGEs-induced cellular dysfunction (Xie et al. 2011; Chen et al. 2017). Cardiac microvascular endothelial cells (CMECs), which are considered as the basis of myocardial microcirculation, play an essential role with respect to cardiac metabolism, growth, apoptosis, muscle contraction, and rhythmicity (Brutsaert 2003). However, few studies focused on the role and regulatory mechanisms of autophagy in CMECs. Obvious morphological and functional difference between macrovascular and microvascular endothelial cells make it hard to speculate the same conclusion in microvascular system. Besides, the microvascular endothelial cells are distinctive from the large vessel endothelial cells not only in shape or size, but also in their response to stress stimulation (Sezer et al. 2018). The mechanism in which AGEs intermediate cytotoxicity and the role of autophagy in AGEs treated CMECs remains to be elucidated.

Nicorandil, a vasodilator acting as both mitochondrial adenosine triphosphate-sensitive potassium channel opener and nitric oxide (NO) donor, is currently used as an antianginal agent (Tarkin and Kaski 2018). Nicorandil was shown to have several beneficial effects on the cardiovascular system, particularly in improving microvascular circulation (Ito et al. 1999) and preventing endothelial dysfunction (Liu et al. 2014). However, whether nicorandil could protect against DM related cardiac microvascular dysfunction is still unknown.

In the present study, we aimed to evaluate the protective role of nicorandil in AGEs treated CMECs and its modulatory mechanisms regarding autophagy.

2. Investigations and results

2.1. Nicorandil protected CMECs against AGEs induced cytotoxicity

AGE-bovine serum albumin (AGE-BSA) significantly reduced cellular proliferation indicated by decreased optical density (OD) value from the Cell Counting Kit-8 (CCK-8) test in a dose-dependent manner ($P< 0.01$) (Fig. 1A). Although three concentrations all reached statistical significance, a widely acknowledged dose of 100 μg/ml (Wang et al. 2016, Li et al. 2017) was selected as working dose in subsequent study. CCK-8 tests suggested that nicorandil at 100 μM ameliorated the AGEs-induced cytotoxicity ($P< 0.01$), and the nicorandil alone group also had an increasing trend in OD value compared with control, although lacking of significance (Fig. 1B). Thus, nicorandil at 100 μM was determined as the optimal work concentration. Correspondingly, AGE-BSA at 100 μg/ml hampered the scratch wound healing process, which indicated that AGE-BSA attenuated cellular migration ($P< 0.01$), and nicorandil was demonstrated to be able to improve cellular migration of CMECs treated with AGE-BSA (Fig. 1C and D).

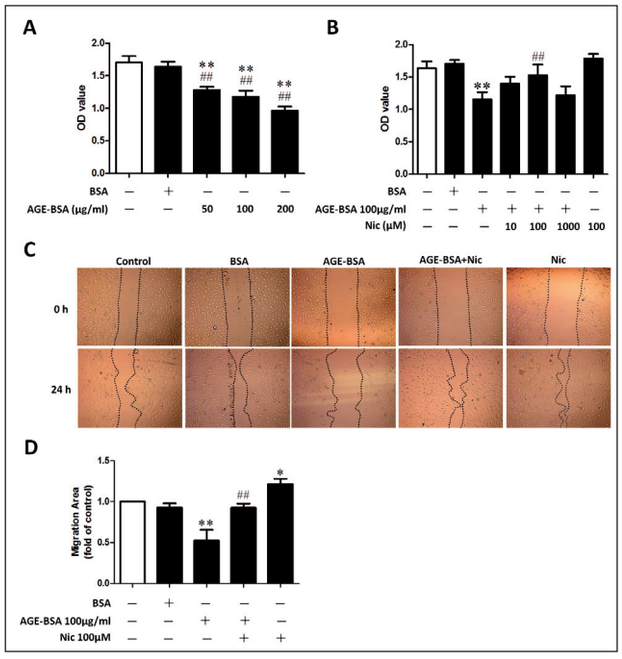

Fig. 1: Nicorandil protected CMECs from AGEs induced cytotoxicity. (A) The results of CCK-8 method in CMECs after incubation with AGE-BSA. (B) The results of CCK-8 method in CMECs after incubation with AGE-BSA (100 μg/ml) and nicorandil. (C, D) Scratch wound healing assay in CMECs treated with AGE-BSA (100 μg/ml) and/or nicorandil (100 μM). The data are shown as the means ± SD (n=6). *P<0.05 vs the control group; ** P<0.01 vs the control group; ## P<0.01 vs the BSA group.

2.2. Chloroquine or wortmannin attenuated the protective effects of nicorandil

Compared with the nicorandil alone group, adding chloroquine dramatically decreased the OD values (Fig. 2A) and impaired scratch wound healing process (Fig. 2B and C). Similarly, adding wortmannin reduced viability of CMECs by CCK-8 assays and impaired scratch wound healing. Either chloroquine or wortmannin alone decreased the OD value and impaired cellular migration. These results suggest that chloroquine or wortmannin could attenuate the protective effects of nicorandil against AGE-induced cytotoxicity.

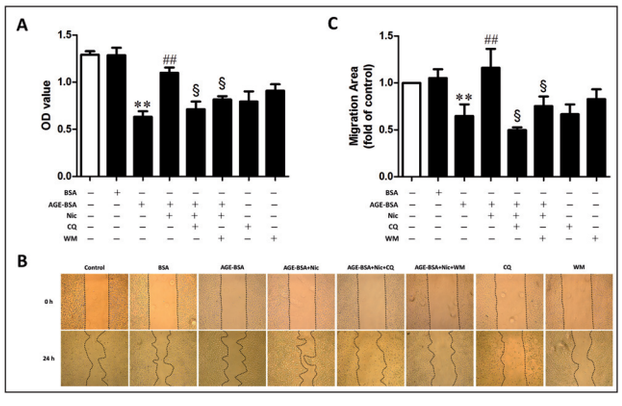

Fig. 2: Chloroquine or wortmannin attenuated the protective effects of nicorandil. (A) The results of CCK-8 method in CMEC models after adding chloroquine (10 μM) or wortmannin (100 nM). (B, C) Scratch wound healing assay in CMEC models after adding chloroquine (10 μM) or wortmannin (100 nM). The data are shown as the means±SD (n=5). ** P<0.01 vs the BSA group; # P<0.05 vs the AGE-BSA group; ## P<0.01 vs the AGE-BSA group.

2.3. Autophagosome formation promoted by nicorandil in CMECs were inhibited by chloroquine or wortmannin

The level of light chain 3 (LC3) -II and the ratio of LC3-II to LC3-I were increased in the AGE-BSA group compared with control. Noteworthily, nicorandil significantly upregulated the expression of LC3-II and the ratio of LC3-II to LC3-I compared with the AGE-BSA group. Furthermore, adding chloroquine increased the expression of LC3-II (Fig. 3A and C). Besides, nicorandil increased phosphorylation of phosphorylated Akt compared with the AGE-BSA group, which was reduced by wortmannin (Fig. 3B and D). Correspondingly, monodansylcadaverine (MDC) – positive CMECs increased in the nicorandil treated group compared the AGE-BSA group, which was attenuated by addition of chloroquine or wortmannin (Fig. 3E). In the same trend, addition of chloroquine or wortmannin decreased intracellular autophagosome formation promoted by nicorandil (Fig. 3F).

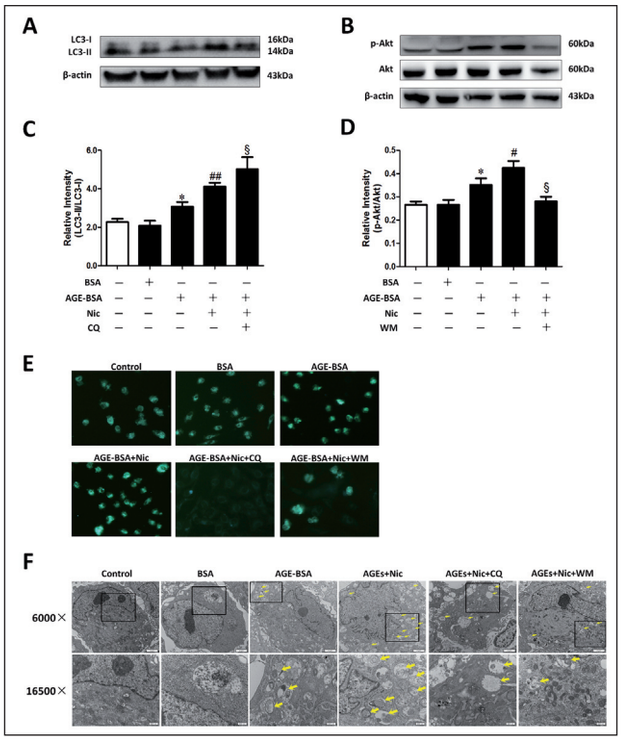

Fig. 3: Autophagosome formation promoted by nicorandil in CMECs was inhibited by chloroquine or wortmannin. (A-D) Western blot analysis of the expression of LC3-II/I and Akt in CMECs. (E) Acidified autophagosomes were shown using MDC fluorescence. (F) Autophagosomes were shown using transmission electron microscopy. Representative electron micrographs at different magnifications (6,000× and 16,500×) were recorded. The data are shown as the means±SD (n=4). ** P<0.01 vs the BSA group; # P<0.05 vs the AGE-BSA group; ## P<0.01 vs the AGE-BSA group; § P<0.05 vs the AGE-BSA + nicorandil group.

2.4. Alagebrium did not suppress autophagosome formation in CMECs induced by nicorandil

Alagebrium, an AGEs cross-link breaker was used to investigate the role of the AGE/RAGE pathway involved in autophagosome formation. Addition of alagebrium did not impact the level of LC3-II or the number of MDC-positive cells (Fig. 4A, B and C). Moreover, the level of RAGE was significantly upregulated by AGE-BSA, and it was reduced by alagebrium, which means alagebrium did affect the AGE/RAGE reaction. However, nicorandil did not regulate RAGE expression. Noteworthily, AGE-BSA group promoted the phosphorylation of p65, which was suppressed by nicorandil (Fig. 4A and B).

2.5. Autophagosome formation promoted by nicorandil was suppressed with PMA

Pyrrolidine dithiocarbamate (PDTC, an inhibitor of nuclear factor-kappa B, NF-κB) upregulated the expression of LC3-II and the ratio of LC3-II to LC3-I compared with the AGE-BSA group, which was in the same trend as the nicorandil group. In addition, the expression of LC3-II

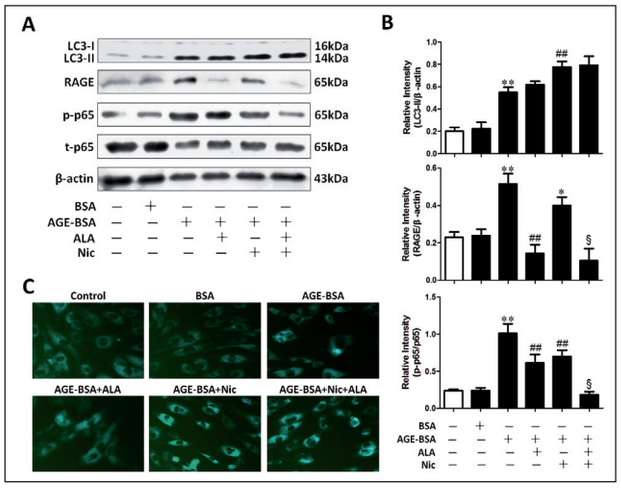

Fig. 4: Alagebrium did not suppress autophagosome formation in CMECs induced by nicorandil. (A, B) Western blot analysis of LC3-II/I, RAGE and Akt in CMECs. (C) Acidified autophagosomes were shown using MDC fluorescence. The data are shown as the means±SD (n=3). ** P<0.01 vs the BSA group; ## P<0.01 vs the AGE-BSA group; § P<0.05 vs the AGE-BSA + nicorandil group.

and the ratio of LC3-II to LC3-I those were promoted by nicorandil were all attenuated by adding phorbol 12-myristate 13-acetate (PMA, a NF-κB activator). AGE-BSA promoted the phosphorylation of the IκB kinase β (IKKβ), IκBα and p65, which was attenuated by either PDTC or nicorandil. In contrast, PMA significantly increased the phosphorylation of IKKβ, IκBα and p65, which indicated NF-κB signaling pathway activation (Fig. 5A and B). Nicorandil or PDTC increased the formation of MDC-labeled acidified autophagosomes in CMECs compared with the AGE-BSA group. In contrast, PMA decreased MDC-labeled acidified autophagosomes (Fig. 5C).

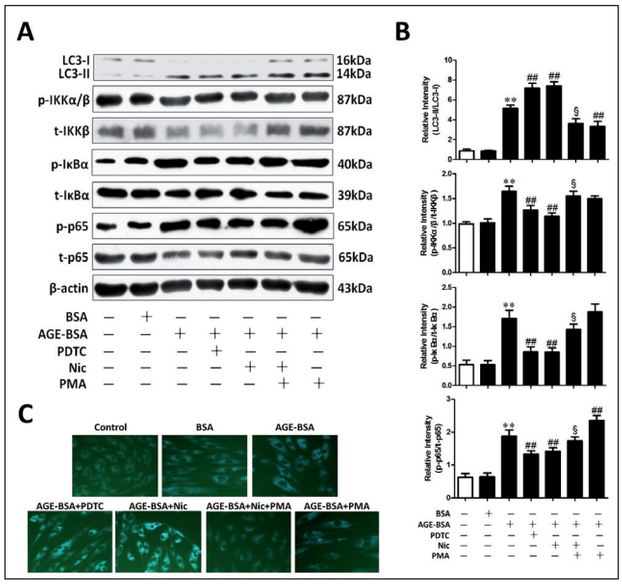

Fig. 5: Autophagosome formation promoted by nicorandil was suppressed by PMA. (A, B) Western blot analysis of LC3-II/I and proteins in NF-κB pathway in CMECs. (C) Acidified autophagosomes were shown using MDC fluorescence. The data are shown as the means±SD (n=4). ** P<0.01 vs the BSA group; ## P<0.01 vs the AGE-BSA group; § P<0.05 vs the AGE-BSA + Nic group.

2.6. Autophagic flux in CMECs induced by nicorandil was attenuated by PMA

As shown in Fig. 6, green fluorescent protein (GFP) and mCherry signals were found in cytoplasm, and yellow puncta (merged by GFP and mCherry fluorescence) were observed, suggesting the formation of early autophagosomes in CMECs exposed to AGE-BSA. Treating CMECs with nicorandil or PDTC resulted in a notable increased number of yellow dots, indicating an increased autophagic flux. However, adding PMA to the nicorandil group significantly reduced the number of yellow dots, indicating an attenuated autophagic flux.

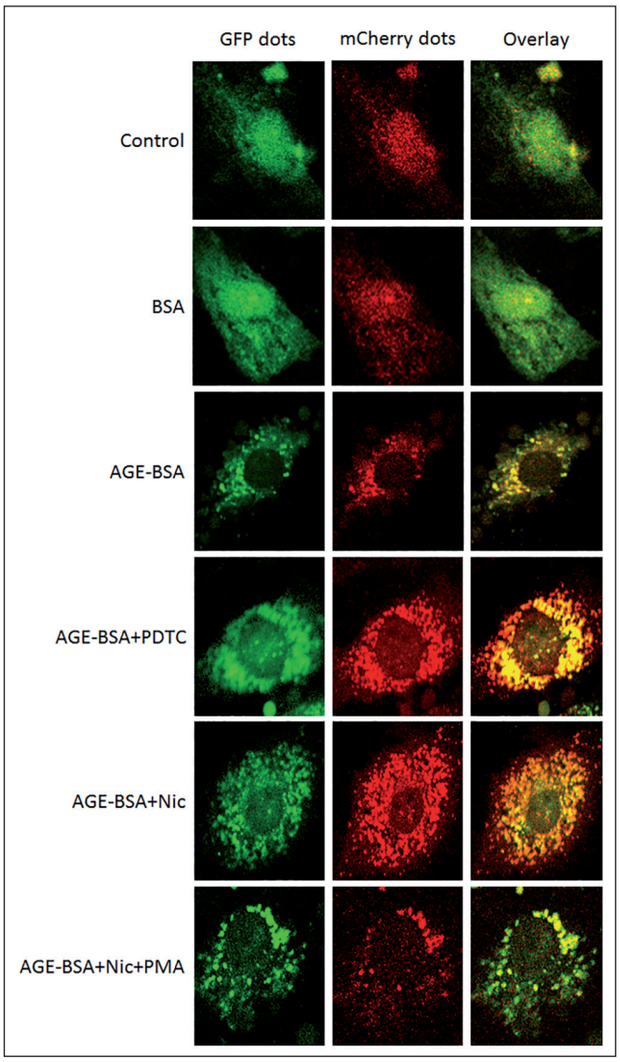

Fig. 6: Autophagic flux in CMECs induced by nicorandil was attenuated by PMA. Representative images of fluorescently LC3 puncta. Green dots and yellow dots represent autophagosomes, and red dots represent autophagosomes and autolysosomes.

3. Discussion

Our results indicated the followings: 1) Nicorandil protected CMECs against AGEs induced cellular impairment, 2) the mechanism in protection by nicorandil was related with autophagy promotion rather than AGE/RAGE interaction, 3) autophagy activation by nicorandil was linked to inhibition of the NF-κB pathway. To our knowledge, this study for the first time demonstrated that nicorandil protects cardiac microvascular endothelium in a diabetic microvascular dysfunction model.

In our previous study (Cui et al. 2014), autophagy activation was demonstrated to be protective in CMECs from ischemia/reperfusion injury. The current study indicated nicorandil promoting autophagy by upregulating LC3-II levels, increasing MDC-positive cells and autophagosome formation. The protective effects of nicorandil were attenuated by lysosomal degradation inhibitor chloroquine, which blocking autophagy flux from the downstream target (Pasquier

2016). Although LC3-II level and autophagosome formation were increased by chloroquine, cellular viability and cellular migration were significantly impaired. Thus, we tested the mechanisms from the other side by blocking the upstream of autophagy using the Class I and III PI3K inhibitor wortmannin (Klionsky et al. 2016). Wortmannin decreased autophagy indicated by less autophagosome formation in transmission electron microscope views and less MDC-positive cells, correspondingly, it increased cytotoxicity and decreased cellular migration. Thus, autophagy activation could be considered as one of the mechanisms in the protection of nicorandil. A similar study found upregulating the levels of LC3-II and p62 protecting HUVECs from AGE-BSA-induced cellular impairment (Chen et al. 2015), which supported our findings.

How AGEs/RAGE activation affects autophagy remains controversial. In our study, we used alagebrium to break cross-links between AGEs/RAGE, which did not alter the levels of LC3-II or autophagosome formation. It was demonstrated that autophagy was upregulated in RAGE knock-out mice subjected to high fat diet (Yu et al. 2017), in contrast, another reports found RAGE short interfering ribonucleic acid (siRNA) abrogated the upregulated autophagy in murine brain capillary endothelial cells (Chan et al. 2018). The receptor-dependent effects of AGE are intermediated via interactions with various proteins such as RAGE as well as AGE-R1, R2, R3, DN-RAGE (Chaudhuri et al. 2018). Additionally, blocking AGEs/RAGE combination also altered the feedback expression of RAGE, thus it seemed that intracellular effects of AGEs were related to the amounts of RAGE expression and the types of other receptors activation depending on different study conditions. This issue needs to be illuminated in future studies.

The receptor-dependent intracellular effects of AGEs mainly rely on the downstream mechanism of the NF-κB pathway (Yang et al. 2019). We found phosphorylation of p65 was promoted in AGEs treated cells, which was abated by nicorandil. A few studies elucidated that inhibiting NF-κB pathway participated in the anti-apopototic mechanisms of nicorandil in pathological models of cardiomyocytes (Su et al. 2018) or pulmonary artery endothelial cells (Wang et al. 2013), which supported our study in similar mechanisms of downregulating p65 expression. However, the cross-talk between autophagy and NF-κB had been debated in various biological processes. A study showed that increment of IKK following with promotion of NF-κB pathway induced autophagosome accumulation in HEK293T cell (Liu et al. 2018), which contradicted our results. Autophagosome accumulation is not able to represent the complete process of autophagy flux. Our study showed that inhibition of NF-κB by PDTC or nicorandil enhanced autophagosome formation, and more importantly promoted autophagic flux measured by Ad-mCherry-GFP-LC3B fusion protein. Previous studies (Djavaheri-Mergny et al. 2006; Xiao 2007) demonstrated NF-κB-mediated autophagosome accumulation, and, although the autophagy flux process was not sufficiently investigated, partly supported our results.

It should be concerned that all our data were generated by using chemical inhibitors. Although these chemicals were all reported in amounts of previous studies, genetic knockdown technique would be more specific approach to further confirm the roles of NF-κB pathway regulation in autophagy. Moreover, the detailed molecular mechanism underlying the regulation of autophagy by AGEs also needs to be further investigated.

In conclusion, our study demonstrated that nicorandil could protect cardiac microvascular endothelial cells from AGEs induced cytotoxicity. Induction of autophagy *via* inhibiting the NF-κB signaling pathway might be involved in the protective mechanisms. The study may provide new insights into developing strategies for the management of diabetic cardiac microvasculature dysfunction.

4. Experimental

4.1. Ethics statements

The current study was approved by Bioethics Committee of Beijing Friendship Hospital affiliated to Capital Medical University. The *in-vitro* study complied with the guidelines and was conducted ethically in accordance with the World Medical Association Declaration of Helsinki. The Human CMECs (Cat. No. 6000) in the study were purchased from ScienCell Research Laboratories (San Diego, CA, USA). The ethical statement of the product was shown on its website, which committed to operating under the highest ethical and legal standards in the acquisition of human and animal tissues used for the preparation of primary cells.

4.2. Materials

Fetal bovine serum (FBS), endothelial cell medium (ECM), endothelial cell growth supplement (ECGS) and penicillin/streptomycin (P/S) solution were purchased from ScienCell Research Laboratories (San Diego, CA, USA). Agents were purchased from manufacturers as following listed. Dulbecco's modified Eagle's medium (DMEM), Life Technologies (Grand Island, NY, USA). AGE-BSA, EMD Millipore Co. (Billerica, MA, USA). Nicorandil, Beijing Sihuankebao Pharmaceutical Co. (Beijing, China). Chloroquine, PDTC and PMA, Sigma-Aldrich Co. (Grand Island, NY, USA). Wortmannin, Life Technologies (Frederick, MD, USA). CCK-8, Dojindo Laboratories (Kumamoto, Japan). Alagebrium, Biopharmaleader Co. (Shanghai, China). Bovine serum albumin (BSA) and adenovirus expressing Ad-mCherry-GFP-LC3B fusion protein, Beyotime Biotechnology (Shanghai, China). The following antibodies with its catalog numbers were purchased from Cell Signaling Technology (Danvers, MA, USA). Anti-LC3 of the microtubule-associated protein (Catalog Number: 3868), anti-phospho-Akt (p-Akt; Ser-473, 4060), anti-Akt (4685), anti-phospho-IKKα/β (2697), anti-IKKβ (8943), anti-phospho-IκBα (2859), anti-IκBα (4812), anti-phospho-NF-κB p65 (3033) or anti-NF-κB p65 (8242) .The anti-β-actin antibody (TA-09) was purchased from Zhongshanjinqiao Biotechnology (Beijing, China).

4.3. Cell culture and disposure

The CMECs were grown in ECM containing 5% FBS, 1% ECGS and 1% P/S solution at 37 °C with 5% carbon dioxide and were subcultured as instructions. CMECs cultured with ECM was designed as a blank control, and the CMECs incubated with non-glycated BSA (100 μg/ml) was designed as a BSA basal control. To investigate the effects of AGEs on CMECs, cells were exposed to different concentrations of AGE-BSA (50, 100, 200 μg/ml) for 24 h. Nicorandil was dissolved in a 0.1% dimethyl sulfoxide solution and was adjusted to concentration of 100mM by adding DMEM, and then it was stored at -20 °C for use in subsequent exposures. To determine the optimal working concentration, the nicorandil solution was adjusted to different concentrations (10, 100 and 1000 μM). Chloroquine at 10 μM (Klionsky et al. 2016) and wortmannin at 100 nM (Wu et al. 2015) as previously described were used to downregulate autophagy in CMECs. PDTC at 50 μM (Wang et al. 2013) or PMA at 1 μM (Shinohara et al. 2005) were used to explore mechanism about NF-κB pathway. CMECs were exposed to above treatments for 24 h before tests.

4.4. Cell viability assay

Cell viability was determined by CCK-8 assay as described in the instructions. After disposure for 24 h in 96-well plates, CMECs were added by 10 μl of CCK-8 liquid to each well. The wells were continuously incubated for 4 h at 37 °C. The absorbance was measured at 450 nm. CMEC proliferation was tested directly based on OD value.

4.5. Scratch wound healing assay

Scratch wound healing assays were implemented as previously reported (Wang et al. 2016, Li et al. 2017). Cellular monolayers were scratched in a straight line by a pipette tip of 200 μl to make a gap between the two parts, and images were acquired under the microscope at 0 and 24 h after scratching. The migration areas were quantified and analyzed with Image J 1.47 software. The migration area was defined as open image area ratio at 24 h to 0 h (Wang et al. 2016; Li et al. 2017). The ratios of migration area in each group to control group area were compared among groups.

4.6. Western blot

Western blotting was performed as described elsewhere (Wu et al. 2015). Generally, cells after treatments were harvested at 4 °C. Cell debris was removed and cytosolic extracts were obtained by centrifugation. The protein samples were heat-denatured after adding loading buffer, and then were electrophoresed and transferred onto a polyvinylidene fluoride membrane. Then the membranes were blocked and were incubated with each indicated primary antibody (1:1000 dilution) overnight at 4 °C. After washing 3 times, the membranes were incubated with peroxidase-conjugated secondary antibodies (1:5000 dilution) for 2 h. Subsequently, the membranes were washed 3 times, and the immunoreactive signals were detected using Western Blotting Imaging System (Clinx Science Instruments Co., Shanghai, China). The band densities were quantified using Image J 1.47 software.

4.7. MDC fluorescence detection

MDC was used to observe acidified autophagosomes at a cellular staining concentration of 50 μM. After the indicated exposures, CMECs were washed and incubated for 15 min with MDC at 37 °C. The cells were washed and fixed with 5% paraformaldehyde for 30 min. The immunostained cells observed immediately and images were acquired using an inverted phase contrast fluorescence microscopy (Leica, Solms, Germany) at an excitation wavelength of 335 nm and an emission wavelength of 525 nm. Each group were captured five random fields at 200 magnification.

4.8. Electron microscopy

The ultrastructural electron microscopy analysis was performed to observe autophagosomes. CMECs were collected after different treatments, and then they were

fixed with 2.5% glutaraldehyde at 4 °C for 3 h in 0.1 M phosphate buffer. Images at different magnifications (6000× and 16,500×) were recorded using a transmission electron microscope (JEOL, Tokyo, Japan).

4.9. Detection of fluorescent LC3 puncta by adenovirus expressing mCherry-GFP-LC3B fusion protein

To detect autophagic flux, CMECs were cultured in 24-well plates and were prepared to be transfected reaching 20%–30% confluence. After two washes, cells were transfected with adenovirus expressing Ad-mCherry-GFP-LC3B at 40 MOI. Twelve hours after transfection, cells were rinsed and then were disposed to different treatments for another 24 h. The expression of mCherry and GFP was visualized with confocal laser scanning microscopy at 400 times magnifications (Leica, Solms, Germany).

4.10. Statistical analysis

Data were obtained from at least three independent tests and were expressed as mean±SD. Statistical analysis was performed using GraphPad Prism 5.01 software (GraphPad Software Inc, La Jolla, CA). Statistical significance was tested by one-way analysis of variance (ANOVA) and Least Significant Difference test was used for post hoc test in ANOVA. P value < 0.05 was considered as statistically significant.

Acknowledgement: We appreciate the technicians in Electron Microscopic Laboratory, Peking University People's Hospital for the assistance of electron microscopic analysis.

Conflicts of interest: The authors declare that there are no conflicts of interest.

Funding: The present study was supported by grants from the National Natural Science Foundation of China (81603425, 81670315), the Beijing Talents Fund (2016000021469G221), the Seed Plan Program of Beijing Friendship Hospital (YYZZ2017A06) and the Beijing Key Clinical Subject Program.

Author contributions: Conceived and designed the study: HH.C., HW.L. and H.C. Analyzed the data: B.H., H.C., WP.L., and HW.L. Performed the studies: B.H. and QB.L. Contributed reagents/materials/analysis tools: WP.L. Wrote the manuscript: B.H. and HH.C. All authors gave final approval and agreed to be accountable for all aspects of work ensuring integrity and accuracy.

References

Brutsaert DL (2003) Cardiac endothelial-myocardial signaling: Its role in cardiac growth, contractile performance, and rhythmicity. Physiol Rev 83: 59–115.

Chan Y, Chen W, Wan W, Chen Y, Li Y, Zhang C (2018) The writing group of the guidelines for monitoring autophagy: Aβ1-42 oligomer induces alteration of tight junction scaffold proteins via RAGE-mediated autophagy in bEnd.3 cells. Exp Cell Res 369: 266–274.

Chaudhuri J, Bains Y, Guha S, Kahn A, Hall D, Bose N, Gugliucci A, Kapahi P (2018) The role of advanced glycation end products in aging and metabolic siseases: bridging association and causality. Cell Metab 28: 337–352.

Chen CH, Chen TH, Wu MY, Chou TC, Chen JR, Wei MJ, Lee SL, Hong LY, Zheng CM, Chiu IJ, Lin YF, Hsu CM, Hsu YH (2017) Far-infrared protects vascular endothelial cells from advanced glycation end products-induced injury via PLZF-mediated autophagy in diabetic mice. Sci Rep 7: 40442.

Chen Y, Du X, Zhou Y, Zhang Y, Yang Y, Liu Z, Liu C, Xie Y (2015) Paeoniflorin protects HUVECs from AGE-BSA-induced injury via an autophagic pathway by acting on the RAGE. Int J Clin Exp Patho 8: 53–62.

Choi AM, Ryter SW, Levine B (2013) Autophagy in human health and disease. N Engl J Med 368: 1845–1846.

Cui H, Li X, Li N, Qi K, Li Q, Jin C, Zhang Q, Jiang L, Yang Y (2014) Induction of autophagy by Tongxinluo through the MEK/ERK pathway protects human cardiac microvascular endothelial cells from hypoxia/reoxygenation injury. J Cardiovasc Pharmacol 64: 180–190.

Djavaheri-Mergny M, Amelotti M, Mathieu J, Besançon F, Bauvy C, Souquère S, Pierron G, Codogno P (2006) NF-kappaB activation represses tumor necrosis factor-alpha-induced autophagy. J Biol Chem 281: 30373–30382.

Ito H, Taniyama Y, Iwakura K, Nishikawa N, Masuyama T, Kuzuya T, Hori M, Higashino Y, Fujii K, Minamino T (1999) Intravenous nicorandil can preserve microvascular integrity and myocardial viability in patients with reperfused anterior wall myocardial infarction. J Am Coll Cardiol 33: 654–660.

Klionsky DJ, Abdelmohsen K, Abe A, Abedin MJ, Abeliovich H, Acevedo Arozena A et al. (2016) Guidelines for the use and interpretation of assays for monitoring autophagy (3rd edition). Autophagy 12: 1–222.

Li Y, Chang Y, Ye N, Dai D, Chen Y, Zhang N, Sun G, Sun Y (2017) Advanced glycation end products inhibit the proliferation of human umbilical vein endothelial cells by inhibiting cathepsin d. Int J Mol Sci 18: E436.

Liu K, Zhang L, Zhao Q, Zhao Z, Zhi F, Qin Y, Cui J (2018) SKP2 attenuates NF-κB signaling by mediating IKKβ degradation through autophagy. J Mol Cell Biol 10: 205–215.

Liu L, Liu Y, Qi B, Wu Q, Li Y, Wang Z (2014) Nicorandil attenuates endothelial VCAM-1 expression via thioredoxin production in diabetic rats induced by streptozotocin. Mol Med Rep 9: 2227–2232.

Pasquier B (2016) Autophagy inhibitors. Cell Mol Life Sci 73: 985–1001.

Ravikumar B, Sarkar S, Davies JE, Futter M, Garcia-Arencibia M, Green-Thompson ZW, Jimenez-Sanchez M, Korolchuk VI, Lichtenberg M, Luo S, Massey DC, Menzies FM, Moreau K, Narayanan U, Renna M, Siddiqi FH, Underwood BR, Winslow AR, Rubinsztein DC (2010) Regulation of mammalian autophagy in physiology and pathophysiology. Physiol Rev 90: 1383–1435.

Sezer M, van Royen N, Umman B, Bugra Z, Bulluck H, Hausenloy DJ, Umman S (2018) Coronary microvascular injury in reperfused acute myocardial infarction: a view from an integrative perspective. J Am Heart Assoc 7: e009949.

Shinohara M, Kawashima S, Yamashita T, Takaya T, Toh R, Ishida T, Ueyama T, Inoue N, Hirata K, Yokoyama M (2005) Xenogenic smooth muscle cell immunization reduces neointimal formation in balloon-injured rabbit carotid arteries. Cardiovasc Res 68: 249–258.

Su Q, Lv X, Sun Y, Ye Z, Kong B, Qin Z (2018) Role of TLR4/MyD88/NF-κB signaling pathway in coronary microembolization-induced myocardial injury prevented and treated with nicorandil. Biomed Pharmacother 106: 776–784.

Tarkin JM, Kaski JC (2018) Nicorandil and Long-acting Nitrates: Vasodilator Therapies for the Management of Chronic Stable Angina Pectoris. Eur Cardiol 13: 23–28.

Wang H, Zuo X, Wang Q, Yu Y, Xie L, Wang H, Wu H, Xie W (2013) Nicorandil inhibits hypoxia-induced apoptosis in human pulmonary artery endothelial cells through activation of mitoKATP and regulation of eNOS and the NF-κB pathway. Int J Mol Med 32: 187–194.

Wang Q, Fan A, Yuan Y, Chen L, Guo X, Huang X, Huang Q (2016) Role of moesin in advanced glycation end Products-Induced angiogenesis of human umbilical vein endothelial cells. Sci Rep 6: 22749.

Wang Y, Zhang ZY, Chen XQ, Wang X, Cao H, Liu SW (2013) Advanced glycation end products promote human aortic smooth muscle cell calcification in vitro via activating NF-κB and down-regulating IGF1R expression. Acta Pharmacol Sin 34: 480–486.

Wu H, Ye M, Yang J, Ding J, Yang J, Dong W, Wang X (2015) Nicorandil protects the heart from Ischemia/Reperfusion injury by attenuating endoplasmic reticulum response-induced apoptosis through PI3K/Akt signaling pathway. Cell Physiol Biochem 35: 2320–2332.

Xiao G (2007) Autophagy and NF-kB: Fight for fate. Cytokine Growth Factor Rev 18: 233–243.

Xie Y, You SJ, Zhang YL, Han Q, Cao YJ, Xu XS, Yang YP, Li J, Liu CF (2011) Protective role of autophagy in AGE-induced early injury of human vascular endothelial cells. Mol Med Rep 4: 459–464.

Yang P, Feng J, Peng Q, Liu X, Fan Z (2019) Advanced glycation end products: potential mechanism and therapeutic target in cardiovascular complications under diabetes. Oxid Med Cell Longev 2019: 9570616.

Yu Y, Wang L, Delguste F, Durand A, Guilbaud A, Rousselin C, Schmidt AM, Tessier F, Boulanger E, Neviere R (2017) Advanced glycation end products receptor RAGE controls myocardial dysfunction and oxidative stress in high-fat fed mice by sustaining mitochondrial dynamics and autophagy-lysosome pathway. Free Radic Biol Med 112: 397–410.